



[60]Fullerene–porphyrin–ferrocene triad self-assembled monolayers (SAMs) for photovoltaic applications



Min Hyung Lee^a, Jung Won Kim^b, Chang Yeon Lee^{c,*}

^a Department of Applied Chemistry, Kyung Hee University, Yongin, Gyeonggi 446–701, Republic of Korea

^b Department of Chemical Engineering, Kangwon National University, 346 Joongang-ro, Samcheok, Gangwon-do 245-711, Republic of Korea

^c Department of Energy and Chemical Engineering, Incheon National University, Incheon 406-772, Republic of Korea

ARTICLE INFO

Article history:

Received 9 January 2014

Received in revised form

20 February 2014

Accepted 26 February 2014

Keywords:

Fullerene

Metal-cluster

Photovoltaic device

Self-assembled monolayer (SAMs)

ABSTRACT

A new triad array, C₆₀–triosmium cluster–zinc porphyrin–ferrocene complex **1**, Os₃C₆₀ZnPfC, was prepared by the decarbonylation of Os₃(CO)₉(μ₃-η²:η²:η²-C₆₀) (**9**) and subsequent reaction with an isocyanide ligand containing porphyrin and ferrocene. This novel triad array exhibits well-defined and stable electrochemical properties in solution due to a robust bonding mode between the C₆₀ and the triosmium cluster. Compound **2**, Os₃C₆₀SiZnPfC was prepared in a manner similar to that of compound **1** from Os₃(CO)₈(CN(CH₂)₃Si(OEt)₃)(μ₃-η²:η²:η²-C₆₀) (**10**) and an isocyanide ligand containing porphyrin and ferrocene. The SAM of triad **2** (**2**/ITO) was fabricated by immersion of an ITO electrode into a chlorobenzene solution of **2** and diazabicyclooctane (2:1 equiv.), and characterized by UV–Vis absorption spectroscopy and cyclic voltammetry. The triad SAM exhibited ideal, well-defined electrochemical responses and high stability due to the stable C₆₀ π-delocalized system via a linkage with the metal cluster center as well as a robust bonding mode. The photoelectrochemical properties of the **2**/ITO triad were investigated by a standard three-electrode system in the presence of an ascorbic acid sacrificial electron donor. Reproducible photocurrent was generated by excitation of the porphyrin moiety in the triad SAM with visible light.

© 2014 Elsevier B.V. All rights reserved.

Introduction

Photoinduced electron transfer (PET) between nanocarbon architecture and photosensitizers has received considerable attention due to its potential applications for optoelectronics, photonics, sensors, and other functional nanoscale molecular devices [1–3]. The chemically functionalized fullerene systems for PET processes often combine with electron donors, such as porphyrin [4–7], ferrocene [8–10], thiophene [11], and carbon nanotubes [12], and additional light harvesting antenna molecules. In these systems, fullerene acts as an efficient electron acceptor because of its intriguing characteristics that allow for the acceleration of photoinduced charge separation and a charge recombination deceleration in the electron transfer process [13]. Numerous molecular donor–acceptor arrays containing accessory pigments, from dyads to hexads, have been synthesized to address the detailed kinetics of energy and electron transfer; in a few cases, these have been successfully applied to solar energy conversion [14–18]. Among them,

a covalently linked fullerene–porphyrin–ferrocene triad system was prepared explosively to obtain a long-lived charge separation state. A lifetime extension can be achieved by the addition of a secondary intermolecular electron transfer to a porphyrin cation radical on the ferrocene, which acts as an additional electron donor in this system. Imahori and coworkers reported long-lived charge separated states of 10 μs in triad systems containing ferrocene, porphyrin, and fullerene [19].

For the purpose of demonstrating a photovoltaic device, molecular donor–acceptor arrays should be immobilized on the various electrodes. Recent progress in covalent fullerene functionalization has led to the advance of electrode-immobilized fullerene and nanocarbon architectures on various surfaces. Numerous electrode-immobilized systems, including porphyrin–fullerene, ferrocene–porphyrin–fullerene triad, ferrocene–porphyrin–fullerene–boron dipyrin tetrad, and organometallic fullerene on gold and indium-tin oxide (ITO) surfaces, have been studied with respect to solar energy conversion [20–26]. However, direct covalent functionalization disturbs the fullerene π-conjugation system by the formation of an σ-bond; therefore, the prepared fullerene SAMs show poorly defined electrochemical properties and instability in reduced states, which causes severe limitations for

* Corresponding author.

E-mail address: cylee@incheon.ac.kr (C.Y. Lee).

technological applications. To address this issue, our group utilized C_{60} -metal cluster complexes with a face-capping $\mu_3-\eta^2:\eta^2:\eta^2-C_{60}$ bonding mode for the immobilization of donor–acceptor arrays on an indium tin oxide (ITO) surface [27,28]. The $\mu_3-\eta^2:\eta^2:\eta^2-C_{60}$ bonding mode stabilizes the C_{60} hybridization such that the intact electrochemical properties of fullerene can be directly transferred to the electrode surface via a linkage to the metal cluster [27].

With our continued interest in photovoltaic devices containing a fullerene–porphyrin–ferrocene triad system, herein we report the preparation of two novel C_{60} –porphyrin–ferrocene triad structures, $Os_3(CO)_8(CNR')(\mu_3-\eta^2:\eta^2:\eta^2-C_{60})$ (**1**, $Os_3C_{60}ZnPfC$) and $Os_3(CO)_7(CNR)(CNR')(\mu_3-\eta^2:\eta^2:\eta^2-C_{60})$ (**2**, $Os_3C_{60}SiZnPfC$) $R = (CH_2)_3Si(OEt)_3$, $R' = ZnPfC$ (Scheme 2). The triosmium cluster moiety in compound **1** links a C_{60} and a porphyrin–ferrocene unit without disturbance of the fullerene π -conjugation system and 3-(triethoxysilyl)propyl isocyanide was acted as a surface anchoring ligand in compound **2**, which is also linked to C_{60} through a triosmium cluster moiety. The triad system forms ideal self-assembled monolayers (SAMs) on the ITO in the presence of diazabicyclooctane (DABCO), which exhibits well-defined electrochemical responses and reproducible photoelectrochemical properties.

Results and discussion

Synthesis and characterization of 1–8

The synthetic methods for isocyanide ligand (**8**, ZnPfC) containing porphyrin and ferrocene are summarized in Scheme 1 and the synthetic routes for triad compounds **1** and **2** are depicted in Scheme 2. The synthetic intermediate **4** was prepared in 50% yield from a dipyrromethane **3** condensation with benzaldehyde in the presence of trifluoroacetic acid, followed by a reduction of the nitro group. Compound **5** was synthesized by esterification of **4** with trifluoroacetic anhydride. Hydrolysis of one of the ester groups of **5** under basic conditions, followed by reductive amination with formylphenyl ferrocene and deprotection of the remaining ester group, afforded compound **7**. Isocyanide functionalized Zn–porphyrin–ferrocene ligand (**8**, ZnPfC) was prepared by a reductive amination reaction of 4-isocyano benzaldehyde with **7** followed by metalation with $Zn(OAc)_2$. Decarbonylation of $Os_3(CO)_9(\mu_3-\eta^2:\eta^2:\eta^2-C_{60})$ (**9**) with $Me_3NO/MeCN$ and subsequent reaction with **8** in chlorobenzene at 60 °C afforded $Os_3(CO)_8(CNR')(\mu_3-\eta^2:\eta^2:\eta^2-C_{60})$ (**1**; $R' = ZnPfC$) in 40% yield. As an alternative, decarbonylation of $Os_3(CO)_8(CN(CH_2)_3Si(OEt)_3)(\mu_3-\eta^2:\eta^2:\eta^2-C_{60})$ (**10**) with $Me_3NO/$

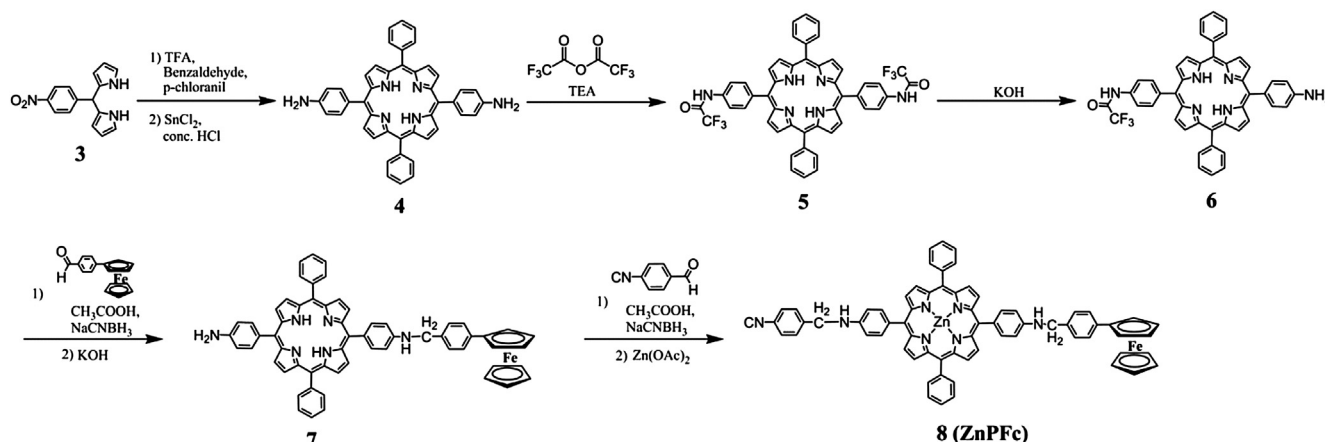
$MeCN$ followed by treatment with **8** in chlorobenzene at 55 °C afforded $Os_3(CO)_7(CNR)(CNR')(\mu_3-\eta^2:\eta^2:\eta^2-C_{60})$ (**2**; $R = (CH_2)_3Si(OEt)_3$, $R' = ZnPfC$) in 50% yield.

Both Compounds **1** and **2** were formulated by molecular ion isotope multiplets (m/z (highest peak): 2613 (**1**); 2814 (**2**)) in the MADI-TOF mass spectrum. The IR spectrum of **1** shows a similar pattern to that of $Os_3(CO)_8(CNCH_2Ph)(\mu_3-\eta^2:\eta^2:\eta^2-C_{60})$ [29], suggesting that the isocyanide ligand in **1** is terminally coordinated at an equatorial site of the Os center. The IR spectrum of **2** exhibits two NC stretches (RNC : 2188 cm^{-1} ; $R'NC$: 2146 cm^{-1}) and an essentially identical CO stretching pattern to that of $Os_3(CO)_7(CNCH_2Ph)_2(\mu_3-\eta^2:\eta^2:\eta^2-C_{60})$ [29], implying that the two isocyanide ligands in **2** occupy equatorial positions on adjacent osmium atoms. The CO stretching bands appear in the typical range of 2080–1950 cm^{-1} , and shift to the low energy region by $\sim 20 cm^{-1}$ as the two isocyanide ligands are coordinated, reflecting the stronger electron-donor effect of the isocyanide ligand relative to the carbonyl ligand (Fig. 1).

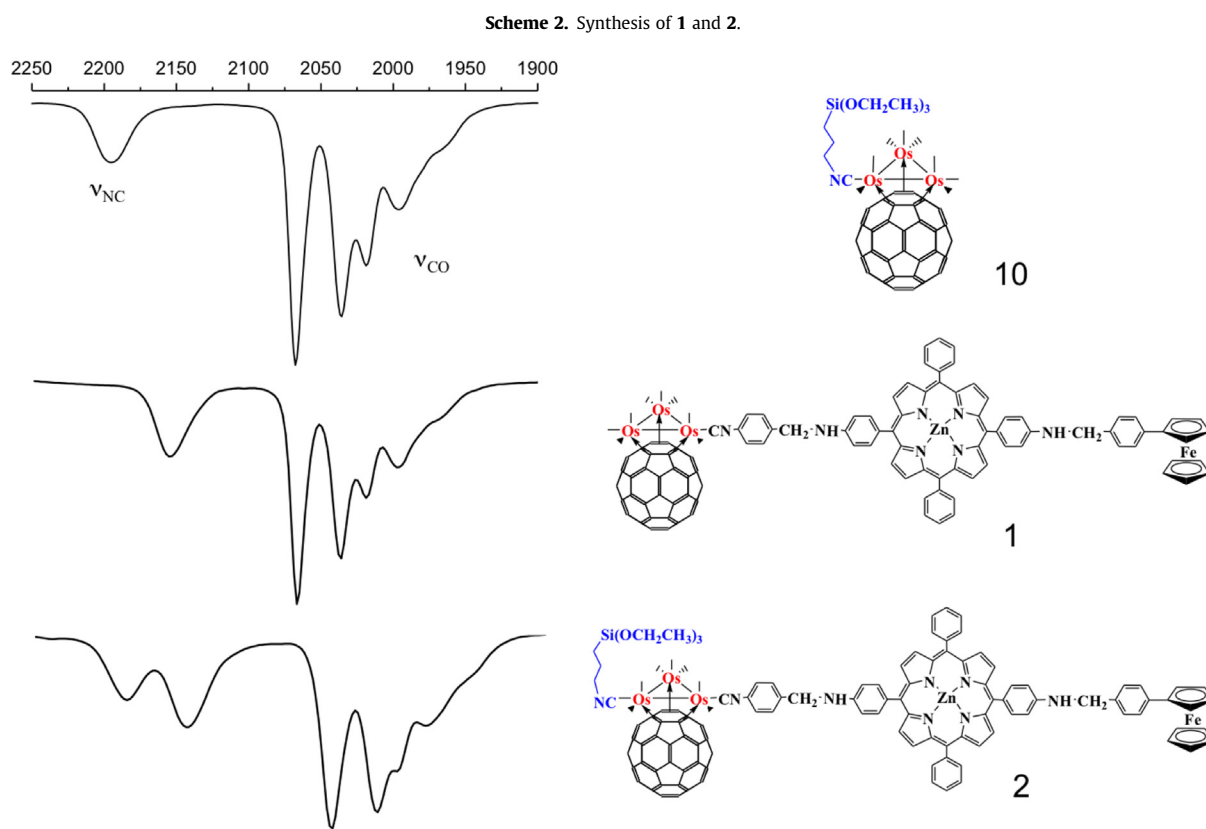
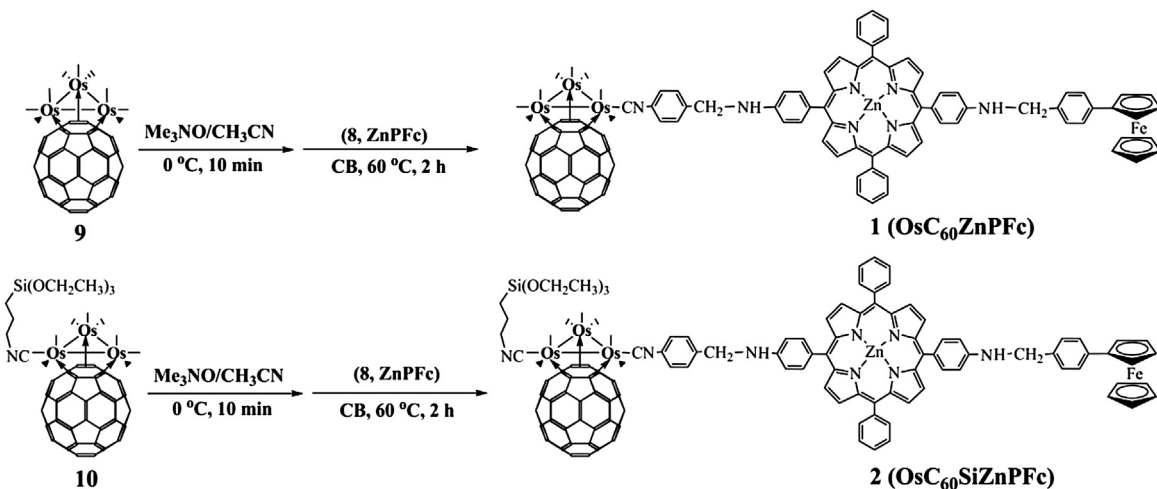
Fig. 2 shows absorption and fluorescence spectra of various chromophores in dichloromethane. Compound **8** exhibits characteristic porphyrin absorption peaks with a strong Soret band at 426 nm and moderate Q bands at 552 and 593 nm. These absorption bands are preserved in compound **1** and additional characteristic broad bands from absorption of the C_{60} moiety appeared between 325 nm and 375 nm. Since there was no significant absorption of ferrocene in the visible region, the porphyrin moiety acts as the primary chromophore for harvesting solar energy in the triad system. The fluorescence spectra of **1** and **8** are provided in Fig. 2b. Porphyrin excitation of **8** at 426 nm in CH_2Cl_2 resulted in typical porphyrin fluorescence with emission maxima at 609 nm and 650 nm. When the porphyrin chromophore of **1** was excited in CH_2Cl_2 , 93% of the porphyrin fluorescence from **1** was quenched by the additional attached fullerene, as compared with **8**. Considering that there was no noticeable fullerene emission in the range of 600–700 nm, this result clearly shows that an efficient electron transfer occurred from ZnP to C_{60} in **1**.

Electrochemical properties of 8, 1, and 2

Solution electrochemical properties of **8**, **1**, and **2** were measured using cyclic voltammetry in chlorobenzene solution with tetrabutylammonium perchlorate as the supporting electrolyte. Cyclic voltammograms (CVs) are depicted in Fig. 3 and the corresponding half-wave potentials ($E_{1/2}$) are listed in Table 1. Compound **8** exhibited two reversible one-electron redox waves in the reduction



Scheme 1. Synthesis of **8**.



region, which were obviously attributed to redox reactions at the zinc porphyrin center. The CV of **10** revealed four reversible one-electron redox waves, with the third and fourth waves overlapping. These overlapping waves have been similarly observed in various known complexes including $\text{Os}_3(\text{CO})_8(\text{PMe}_3)(\mu_3\text{-}\eta^2\text{:}\eta^2\text{:}\eta^2\text{-C}_{60})$ and $\text{Os}_3(\text{CO})_{9-n}(\text{CNCH}_2\text{Ph})_n(\mu_3\text{-}\eta^2\text{:}\eta^2\text{:}\eta^2\text{-C}_{60})$ ($n = 2, 3,$ and 4) [29], due to C_{60} reductions combined with electronic communication between C_{60} and the metal cluster centers. As expected, the general feature of the CV of **1** was the sum of those of **8** and **10**. The **1** CV showed seven redox waves that consisted of five reversible redox waves corresponding to redox reactions at the C_{60} center and two reversible redox waves corresponding to the porphyrin center. Although the CV of **2** was similar to that of **1**, the C_{60} center redox potential in **2** was shifted in the negative direction with preserved

redox potentials of the porphyrin center, reflecting the electron-donor nature of the isocyanide ligand. The CVs of **1** and **2** in the oxidation region exhibited three reversible one-electron oxidation waves (see [Supplementary data](#)). The first one-electron oxidation was assigned to the oxidation of ferrocene, whereas the second and third oxidations were assigned to a stepwise abstraction of two electrons from the porphyrin center.

Formation and photovoltaic properties of **2**/ITO SAM

The SAM of **2** (**2**/ITO) was prepared by the immersion of an ITO electrode into a chlorobenzene solution of **2** and DABCO (2:1 equiv.) at $100\text{ }^\circ\text{C}$ for 7 h, followed by washing with chlorobenzene and dichloromethane ([Scheme 3](#)). The presence of DABCO in the SAM

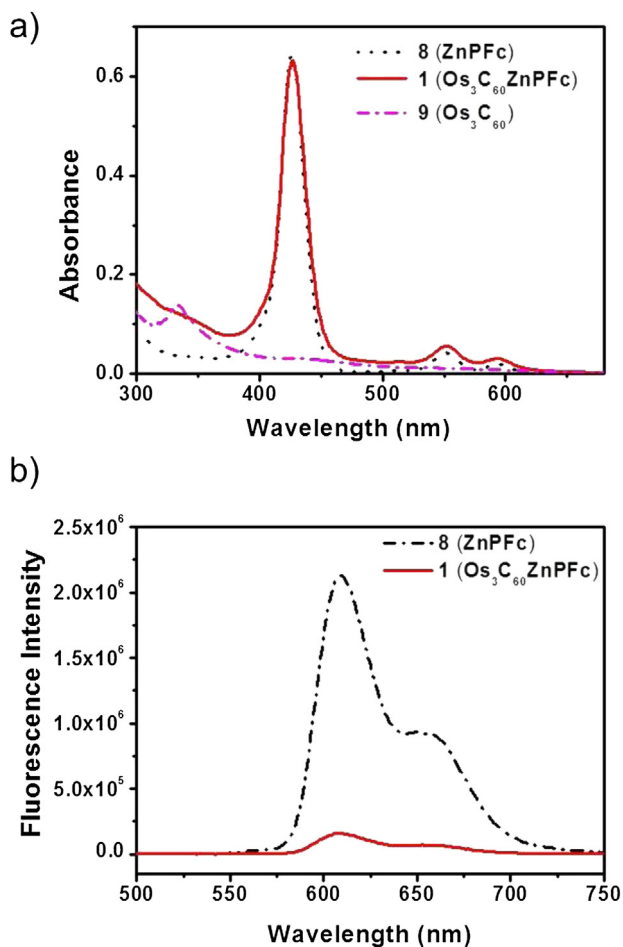


Fig. 2. a) UV–Vis spectra of **1**, **8**, and **9** in CH_2Cl_2 . b) Fluorescence spectra of **1** and **8** in CH_2Cl_2 with excitation at 426 nm.

formation resulted in a well-ordered structural confinement due to the strong interaction between ZnP and the bifunctional DABCO base, which may lead to high surface coverage as shown in previously reported studies [17,28]. The absorption spectrum of **2**/ITO (Fig. 5) showed a characteristic solet (438 nm) band, which was broader and red-shifted by ~ 12 nm compared with that of **2** in solution due to stacking of the porphyrin moieties on the surface. The CV of **2**/ITO (Fig. 4) in deoxygenated dichloromethane exhibited three well resolved and electrochemically stable redox waves at -1.21 , -1.52 , and -2.02 V ($E_{1/2}$) with a relative area of 1:1:3.2. Importantly, the overall features of the **2**/ITO CV were similar to that of **2** in solution. The first and second waves were successive, one-electron reductions of **2** localized on C_{60} . The third wave corresponded to an overlapping pattern of two-electron reductions of the C_{60} –triosmium cluster moiety and one electron reduction of the porphyrin moiety. Three successive waves due to the oxidation of ferrocene and the porphyrin moiety were also observed at 0, 0.19, and 0.38 V ($E_{1/2}$) for **2**/ITO (see Supplementary data). The monolayer surface coverage (Γ) of **2**/ITO was estimated as 1.8×10^{-10} mol cm^{-2} from the integrated charge of the first reduction peak at -1.21 V, which was comparable to $\sim 1.9 \times 10^{-10}$ mol cm^{-2} for a closed packed monolayer of C_{60} . The ideal, well-defined electrochemical responses in **2**/ITO may be ascribed to the fact that π -delocalization of C_{60} was not perturbed by the π -type coordination of C_{60} on the metal cluster and the C_{60} moiety remained intact during SAM formation by confining the C_{60} –metal cluster complex to the electrode surface via a linkage to the metal center.

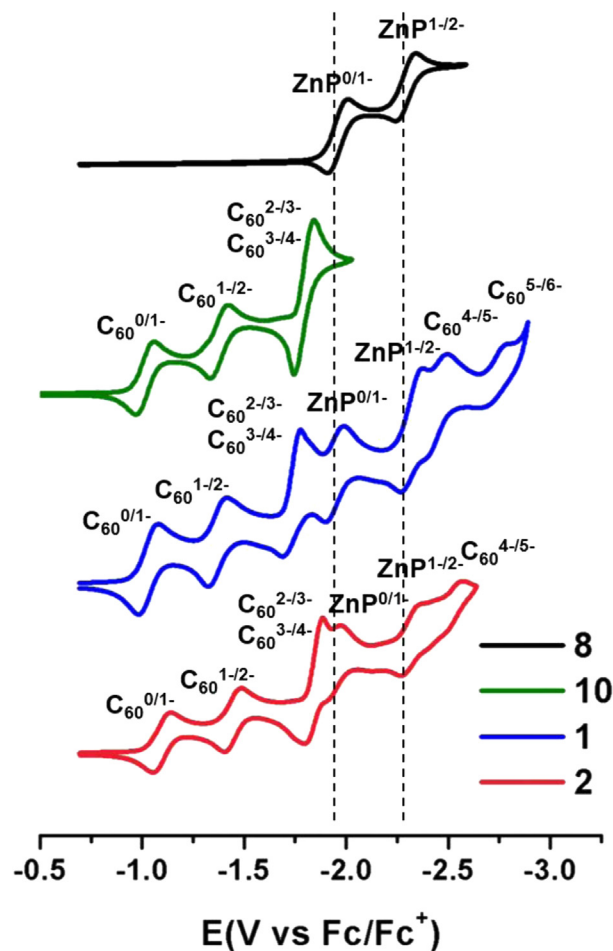


Fig. 3. Cyclic voltammograms of **8**, **10**, **1**, and **2** in dry, deoxygenated chlorobenzene (0.1 M $[(n\text{-Bu})_4\text{N}][\text{ClO}_4]$) at a scan rate of 10 mV/s.

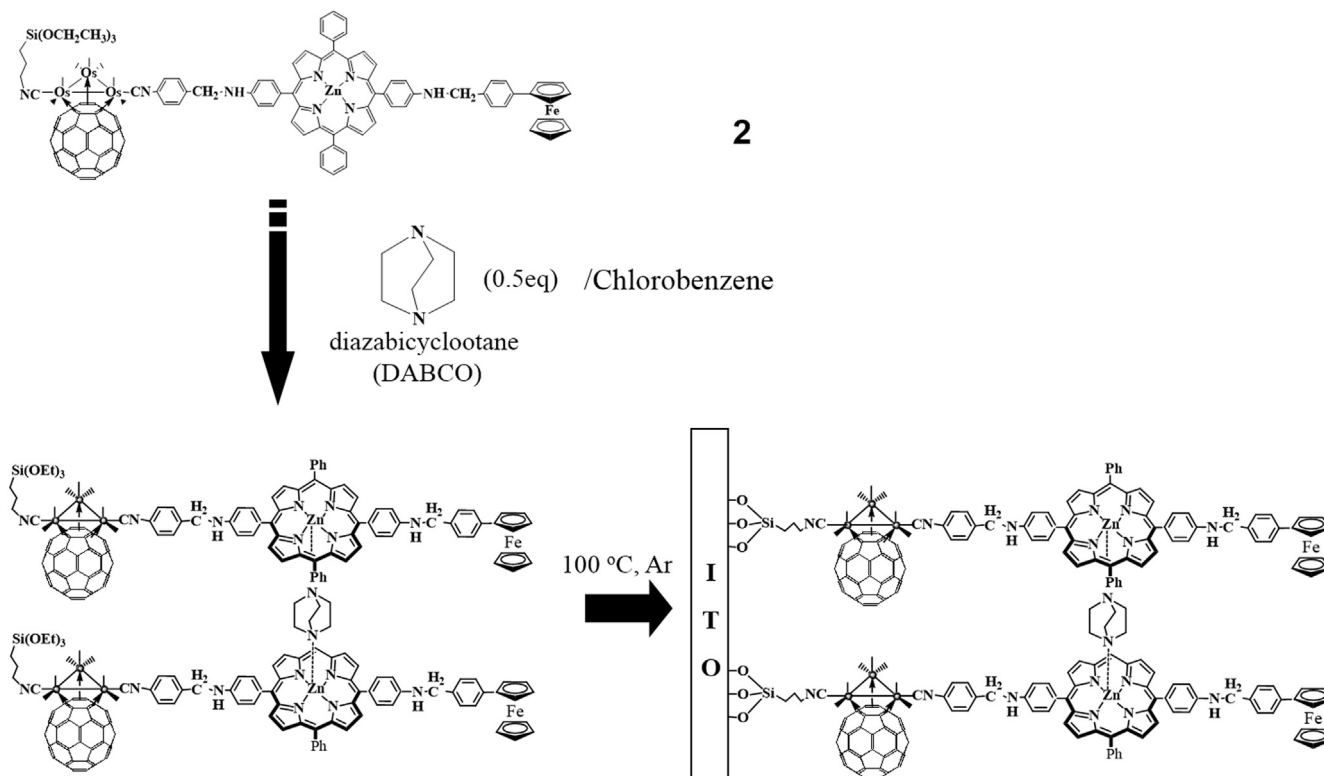
Photocurrent measurement was carried out for **2**/ITO in a 0.1 M Na_2SO_4 solution containing 50 mM ascorbic acid (AsA) as an electron sacrifier by the three electrode system of the modified ITO substrate as a working electrode, a Pt counter electrode, and a Ag/AgCl (3 M NaCl) reference electrode, denoted as 'ITO/**2**/AsA/Pt'. The solution was controlled at pH 3.5. A stable anodic photocurrent was observed immediately upon irradiation of the ITO electrode with $\lambda = 435$ nm light (0.96 mW cm^{-2}) at an applied potential of 100 mV and the response was reversibly repeated, as shown in Fig. 6. The ITO/**2**/AsA/Pt cell action spectrum (solid blue line with circles in Fig. 5) matched well with the absorption spectrum of **2**/ITO in the 380–700 nm region, indicating that the porphyrin unit acted as a real photoactive center for photocurrent generation. The quantum yield was estimated to be 11% for **2**/ITO, based on the amount of photons absorbed by the chromophores.

Concluding remarks

We prepared a new triad system containing C_{60} , porphyrin, and ferrocene using a triosmium cluster as a linker. The triad array exhibited well-defined and stable electrochemical properties in solution due to robust bonding between C_{60} and the triosmium cluster. We also successfully constructed a highly ordered, nearly fully covered [60]fullerene triosmium cluster–zinc porphyrin–ferrocene triad SAM on the ITO surface with the aid of DABCO. The triad SAM exhibited ideal, well-defined electrochemical responses and high stability due to the stability of the C_{60} π -delocalized

Table 1
Half-wave potential ($E_{1/2}$ vs. E_0 (Fc/Fc⁺)) in C₆₀, **8**, **1**, **2**, and 2/ITO CVs.

Compound	ZnP ^{+2/+}	ZnP ^{0/+}	Fc ^{0/+}	C ₆₀ ^{0/-}	C ₆₀ ^{2-/-}	C ₆₀ ^{2-/3-}	C ₆₀ ^{3-/4-}	ZnP ^{0/-}	ZnP ^{-2/-}	C ₆₀ ^{4-/5-}	C ₆₀ ^{5-/6-}	Solvent
C ₆₀				-1.06	-1.43	-1.91	-2.38					CB
8												CB
1	0.29	0.12	0	-1.03	-1.37	-1.73		-1.96	-2.29	-2.44	-2.73	CB
2	0.29	0.14	0	-1.10	-1.45	-1.84		-1.94	-2.32	-2.53		CB
SAM	ZnP ^{+2/+}	ZnP ^{0/+}	Fc ^{0/+}	C ₆₀ ^{0/-}	C ₆₀ ^{2-/-}	C ₆₀ ^{2-/3-}	C ₆₀ ^{3-/4-}	ZnP ^{0/-}	ZnP ^{-2/-}	C ₆₀ ^{4-/5-}	C ₆₀ ^{5-/6-}	Solvent
2/ITO	0.38	0.19	0	-1.21	-1.52	-2.02						DM
												2/ITO



Scheme 3. Preparation of 2/ITO.

system via a linkage to the metal cluster center as well as a robust bonding mode between C₆₀ and the metal cluster. The photovoltaic cell based on the triad SAMs revealed a reproducible and stable photocurrent when it was irradiated by visible light. The present successful application of C₆₀-metal cluster complexes in photo

electrochemical cells promises other useful technological applications of C₆₀-metal cluster based SAMs for molecular electronic device fabrication. Efforts are currently underway using these triad and triad-based SAMs to investigate the detailed kinetics involved in electron transfer in solution and on electrodes.

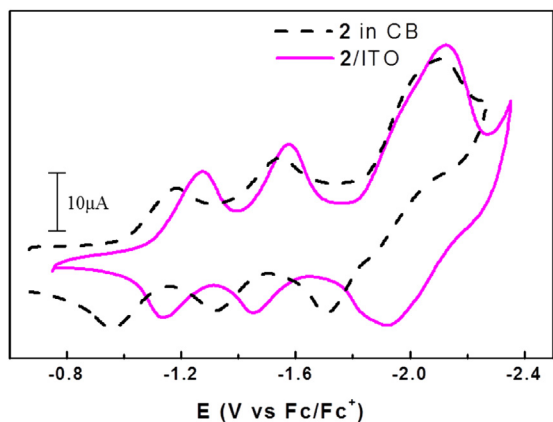


Fig. 4. Cyclic voltammograms of **2** (dashed line) and **2/ITO** (solid line) containing 0.1 M Bu₄NPF₆ as an electrolyte (scan rate = 0.5 V s⁻¹).

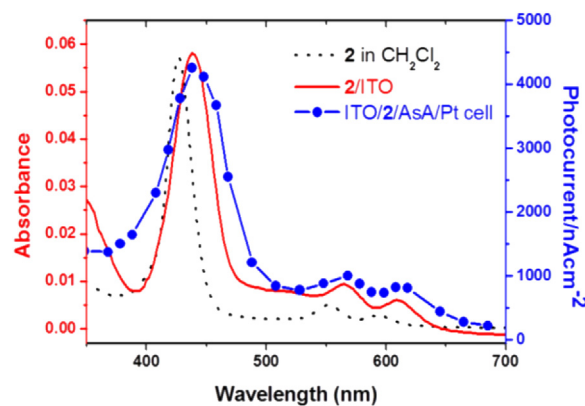


Fig. 5. Absorption spectrum of **2/ITO** (solid red line) and action spectrum of ITO/**2/AsA/Pt** (solid blue line with circles) with 0.7 mW cm⁻² light; applied potential, 100 mV vs. Ag/AgCl (3 M NaCl). (For interpretation of the references to color in this figure legend, the reader is referred to the web version of this article.)

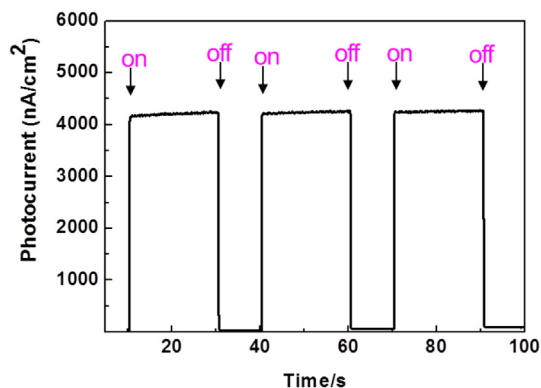


Fig. 6. Photocurrent response of ITO/2/AsA/Pt irradiated with 435 nm light (0.96 mW cm^{-2}); applied potential, 100 mV vs. Ag/AgCl (3 M NaCl).

Experimental section

General comments

All reactions were carried out under a nitrogen atmosphere with the use of standard Schlenk techniques. Solvents were dried over appropriate drying agents and distilled immediately before use. C_{60} (99.5%, Southern Chemical Group, LLC.) was used without further purification. Anhydrous trimethylamine *N*-oxide (m.p. 255–230 °C) was obtained from $\text{Me}_3\text{NO} \cdot 2\text{H}_2\text{O}$ (98%, Aldrich) by sublimation (three times) at 90–100 °C under vacuum. Dipyrromethane **3** [30] and $\text{Os}_3(\text{CO})_8(\text{CN}(\text{CH}_2)_3\text{Si}(\text{OEt})_3)(\mu_3-\eta^2:\eta^2:\eta^2-\text{C}_{60})$ [27] were prepared according to published methods. Infrared spectra were obtained on a Bruker EQUINOX-55 FT-IR spectrophotometer. ^1H (400 MHz) NMR spectra were recorded on a Bruker AVANCE-400 spectrometer. Positive ion FAB mass spectra (FAB^+) and MALDI-TOF were obtained at the Korea Basic Science Institute.

Synthesis of 1–8

Synthesis of 4

A solution of dipyrromethane **3** (2 g, 7.48 mmol) and benzaldehyde (0.794 g, 7.48 mmol) in chloroform (750 mL) was degassed by bubbling with nitrogen for 1 h. The reaction vessel was shielded from ambient light. Trifluoroacetic acid (1.04 mL, 7.48 mmol) was then added to one portion. The solution was stirred for 2 h at room temperature under a nitrogen atmosphere. To the reddish black reaction mixture, *p*-chloranil (2.76 g, 11.2 mmol) was added with overnight stirring. Triethylamine was added and then the reaction mixture was concentrated. Flash column chromatography on silica gel (CH_2Cl_2) yielded the desired porphyrin from the mixture as the third major band. Reprecipitation with chloroform–methanol afforded a vivid reddish purple solid. SnCl_2 (1.5 g, 7.9 mmol) was added to a suspension of the above crude product (550 mg, 0.780 mmol) in concentrated HCl solution (116 mL). The reaction mixture was stirred for 45 min at room temperature and maintained at 95–100 °C for an additional 30 min. After cooling, the reaction was quenched by the slow addition of 25% ammonia. The organic layer was extracted with CHCl_3 and washed with water. After standing over anhydrous Na_2SO_4 , the organic extract was concentrated to dryness. Flash column chromatography on silica gel with CH_2Cl_2 –ethyl acetate (30:1) as the eluent and subsequent reprecipitation from CHCl_3 – CH_3OH gave **4** as a deep violet solid (200 mg, 0.283 mmol, 4%). ^1H NMR (400 MHz, CDCl_3) δ –2.75 (br s, 2H), 3.99 (br s, 4H), 7.03 (d, $J = 8.3 \text{ Hz}$, 4H), 7.74 (m, 6H), 7.98 (d, $J = 8.3 \text{ Hz}$, 4H), 8.21 (d, $J = 9.3 \text{ Hz}$, 4H), 8.81 (d, $J = 4.8 \text{ Hz}$, 4H), 8.92 (d, $J = 4.8 \text{ Hz}$, 4H). MS (FAB^+) m/z 645 $[\text{M} + \text{H}]^+$.

Synthesis of 5

A portion of **4** (200 mg, 0.283 mmol), triethylamine (0.1 mL, 0.849 mmol), and trifluoroacetic anhydride (178 mg, 0.849 mmol) were stirred in chloroform (20 mL) at room temperature for 20 min. TLC analysis indicated total consumption of the starting material. The reaction mixture was quenched with water and extracted with chloroform, and extracts were dried (Na_2SO_4). The solvent was removed by evaporation at reduced pressure and the crude product was purified by flash column chromatography on silica gel with hexane–ethyl acetate (2:1) as the eluent to give 213 mg (90%) of the desired compound. ^1H NMR (400 MHz, CDCl_3) δ –2.74 (br s, 2H), 7.76 (m, 6H), 7.97 (d, $J = 8.3 \text{ Hz}$, 4H), 8.18 (d, $J = 6.2 \text{ Hz}$, 4H), 8.24 (d, $J = 8.3 \text{ Hz}$, 4H), 8.29 (s, 2H), 8.80 (d, $J = 4.8 \text{ Hz}$, 4H), 8.85 (d, $J = 4.8 \text{ Hz}$, 4H). MS (FAB^+) m/z 837 $[\text{M} + \text{H}]^+$.

Synthesis of 7

Compound **5** (320 mg, 0.382 mmol) was dissolved in a mixture of 35 mL methanol, 20 mL THF, and 2 mL of aqueous 10% KOH. The reaction mixture was stirred at 75 °C for 90 min, after which it was poured into a separatory funnel containing water (50 mL). The aqueous phase was extracted with chloroform and extracts were dried (Na_2SO_4). The solvent was removed by evaporation at reduced pressure and the crude product was purified by flash column chromatography on silica gel with hexane–ethyl acetate (1:1) as the eluent to give 141 mg (50%) of the desired compound **6**. Five drops of acetic acid (96%) were added to an ethanol solution (40 mL) of **6** (170 mg, 0.229 mmol), 4-formylphenylferrocene (73.0 mg, 0.252 mmol), and anhydrous Na_2SO_4 at room temperature and then the reaction mixture was stirred at reflux for 2 h. After evaporation of the solvent *in vacuo*, the residue was redissolved in THF/MeOH (1/1, 40 mL). To the resulting solution, a 1.0 M THF solution (0.688 mL) of NaBH_3CN was added at 0 °C for 15 min. The solvent was evaporated and the residue was purified by column chromatography (silica gel, hexane/ethyl acetate = 2:1) to afford a deep violet solid. The obtained violet solid (150 mg, 0.148 mmol) was dissolved in a mixture of 20 mL methanol, 10 mL THF, and 2 mL of aqueous 10% KOH. The reaction mixture was stirred at 75 °C for 90 min, after which it was poured into a separatory funnel containing water (20 mL). The aqueous phase was extracted with chloroform and extracts were dried (Na_2SO_4). The solvent was removed by evaporation at reduced pressure and the crude product was purified by flash column chromatography on silica gel with hexane–ethyl acetate (2:1) as the eluent to give 120 mg (90%) of **7**. ^1H NMR (400 MHz, $\text{THF}-d_8$) δ –2.59 (s, 2H), 4.01 (s, 5H), 4.29 (t, $J = 1.7 \text{ Hz}$, 2H), 4.49 (d, $J = 5.5 \text{ Hz}$, 2H), 4.69 (t, $J = 1.7 \text{ Hz}$, 2H), 4.94 (s, 2H), 5.82 (t, $J = 5.5 \text{ Hz}$, 1H), 6.98 (d, $J = 8.3 \text{ Hz}$, 2H), 7.04 (d, $J = 8.3 \text{ Hz}$, 2H), 7.45 (d, $J = 8.1 \text{ Hz}$, 2H), 7.55 (d, $J = 8.1 \text{ Hz}$, 2H), 7.75 (m, 6H), 7.88 (d, $J = 8.3 \text{ Hz}$, 2H), 7.95 (d, $J = 8.3 \text{ Hz}$, 2H), 8.21 (m, 4H), 8.77 (d, $J = 4.5 \text{ Hz}$, 4H), 8.94 (d, $J = 4.5 \text{ Hz}$, 4H). MS (FAB^+) m/z 798 $[\text{M} + \text{H}]^+$.

Synthesis of 8

Five drops of acetic acid (96%) were added to a THF solution (40 mL) of **7** (220 mg, 0.239 mmol), 4-isocyanobenzaldehyde (38.0 mg, 0.362 mmol), and anhydrous Na_2SO_4 at room temperature, and then the reaction mixture was stirred at reflux for 2 h. After evaporation of the solvent *in vacuo*, the residue was redissolved in THF/MeOH (1/1, 40 mL). To the resulting solution, a 1.0 M THF solution (0.718 mL) of NaBH_3CN was added at 0 °C for 15 min. The solvent was evaporated and the residue was purified by column chromatography (silica gel, CH_2Cl_2 /methanol = 99:1) to afford a deep violet solid. A 5 mL saturated methanol solution of $\text{Zn}(\text{OAc})_2$ (87.5 mg, 0.477 mmol) was added to a CHCl_3 solution (40 mL) of violet solid, which was obtained from the above reaction, at room temperature and the resulting solution was stirred for 30 min. The solvent was evaporated and the residue was purified by column

chromatography (silica gel, CH₂Cl₂/methanol = 99:1). Recrystallization from THF/hexane resulted in **8** as a purple crystalline solid (160 mg, 0.146 mmol, 61%). δ 4.02 (s, 5H), 4.29 (t, $J = 1.7$ Hz, 2H), 4.50 (d, $J = 5.3$ Hz, 2H), 4.54 (d, $J = 5.7$ Hz, 2H), 4.69 (t, $J = 1.7$ Hz, 2H), 5.70 (t, $J = 5.5$ Hz, 1H), 5.85 (t, $J = 5.8$ Hz, 1H), 6.93 (d, $J = 8.3$ Hz, 2H), 7.03 (d, $J = 8.3$ Hz, 2H), 7.46 (d, $J = 8.1$ Hz, 4H), 7.55 (d, $J = 8.1$ Hz, 2H), 7.59 (d, $J = 8.1$ Hz, 2H), 7.72 (m, 6H), 7.92 (d, $J = 8.3$ Hz, 2H), 7.95 (d, $J = 8.3$ Hz, 2H), 8.21 (m, 4H), 8.82 (m, 4H), 8.94 (d, $J = 4.6$ Hz, 2H), 8.99 (d, $J = 4.6$ Hz, 2H). MS (FAB⁺) m/z 975 [M + H]⁺.

Synthesis of Os₃(CO)₈(CNR')(μ_3 - η^2 : η^2 -C₆₀) (**1**; R' = ZnPF₆)

An acetonitrile solution (1.2 mL) of anhydrous Me₃NO (5.35 mg, 0.071 mmol) was added dropwise to a chlorobenzene solution (60 mL) of Os₃(CO)₉(μ_3 - η^2 : η^2 -C₆₀) (100 mg, 0.064 mmol) at 0 °C. The reaction mixture was allowed to warm to room temperature for 40 min. After evaporation of the solvent *in vacuo*, the residue was dissolved in chlorobenzene (60 mL). A chlorobenzene solution of **8** (71.1 mg, 0.065 mmol) was added to the resulting solution and the reaction mixture was stirred at 60 °C for 2 h. The solvent was evaporated and the residue was purified by column chromatography (silica gel, CS₂:CH₂Cl₂, 1:3) to result in compound **1** (67.7 mg, 0.026 mmol, 40%) as a brown solid. IR (CH₂Cl₂) ν (NC) 2155(m); ν (CO) 2067(vs), 2037(s), 2019(s), 1997(m) cm⁻¹; ¹H NMR (400 MHz, CDCl₃) δ 4.01 (s, 5H), 4.29 (t, $J = 1.7$ Hz, 2H), 4.51 (d, $J = 5.4$ Hz, 2H), 4.58 (d, $J = 5.6$ Hz, 2H), 4.70 (t, $J = 1.7$ Hz, 2H), 5.72 (t, $J = 5.5$ Hz, 1H), 5.91 (t, $J = 5.8$ Hz, 1H), 6.90 (d, $J = 8.3$ Hz, 2H), 7.03 (d, $J = 8.3$ Hz, 2H), 7.43 (d, $J = 8.4$ Hz, 2H), 7.48 (d, $J = 8.1$ Hz, 2H), 7.56 (d, $J = 8.1$ Hz, 2H), 7.63 (d, $J = 8.4$ Hz, 2H), 7.71 (m, 6H), 7.89 (d, $J = 8.3$ Hz, 2H), 7.95 (d, $J = 8.3$ Hz, 2H), 8.18 (m, 4H), 8.76 (d, $J = 4.6$ Hz, 2H), 8.78 (d, $J = 4.6$ Hz, 2H), 8.87 (d, $J = 4.6$ Hz, 2H), 8.96 (d, $J = 4.6$ Hz, 2H). MALDI-TOF m/z 2613 [M]⁺.

Synthesis of Os₃(CO)₇(CNR)(CNR')(μ_3 - η^2 : η^2 -C₆₀) (**2**); R = (CH₂)₃Si(OEt)₃, R' = ZnPF₆)

An acetonitrile solution (1 mL) of anhydrous Me₃NO (4.70 mg, 0.063 mmol) was added dropwise to a chlorobenzene solution (60 mL) of Os₃(CO)₈(CN(CH₂)₃Si(OEt)₃)(μ_3 - η^2 : η^2 -C₆₀) (100 mg, 0.057 mmol) at 0 °C. The reaction mixture was allowed to warm to room temperature for 40 min. After evaporation of the solvent *in vacuo*, the residue was dissolved in chlorobenzene (60 mL). A chlorobenzene solution of **8** (62.6 mg, 0.057 mmol) was added to the resulting solution and the reaction mixture was stirred at room temperature for 2.5 h. The solvent was evaporated and the residue was purified by column chromatography (silica gel, CS₂:CH₂Cl₂, 1:2) to result in compound **2** (80.3 mg, 0.029 mmol, 50%) as a brown solid. IR (CH₂Cl₂) ν (NC) 2188(m), 2146(m); ν (CO) 2047(vs), 2016(s), 2001(s), 1983(m) cm⁻¹; ¹H NMR (400 MHz, CDCl₃) δ 0.65 (m, 2H), 1.15 (t, $J = 7.0$ Hz, 9H), 1.79 (m, 2H), 3.75 (q, $J = 7.0$ Hz, 6H), 3.98 (t, $J = 6.7$ Hz, 2H), 4.01 (s, 5H), 4.29 (t, $J = 1.7$ Hz, 2H), 4.51 (d, $J = 5.4$ Hz, 2H), 4.56 (d, $J = 5.6$ Hz, 2H), 4.69 (t, $J = 1.7$ Hz, 2H), 5.70 (t, $J = 5.5$ Hz, 1H), 5.86 (t, $J = 5.8$ Hz, 1H), 6.92 (d, $J = 8.3$ Hz, 2H), 7.03 (d, $J = 8.3$ Hz, 2H), 7.41 (d, $J = 8.4$ Hz, 2H), 7.47 (d, $J = 8.1$ Hz, 2H), 7.55 (d, $J = 8.1$ Hz, 2H), 7.61 (d, $J = 8.4$ Hz, 2H), 7.72 (m, 6H), 7.93 (d, $J = 8.3$ Hz, 2H), 7.97 (d, $J = 8.3$ Hz, 2H), 8.20 (m, 4H), 8.80 (m, 4H), 8.91 (d, $J = 4.6$ Hz, 2H), 8.98 (d, $J = 4.6$ Hz, 2H). MALDI-TOF m/z 2814 [M]⁺.

Preparation of **2**/ITO

ITO (indium-tin-oxide) glass was cleaned with acetone and dried by blowing a N₂ stream over the surface. The ITO electrode was immersed in a chlorobenzene solution containing **2** and diazabicyclooctane (DABCO) at a total concentration of 1 mM (molar ratio of **2**:DABCO = 2:1) at 100 °C for 7 h under an argon atmosphere. The substrates were rinsed and sonicated in pure chlorobenzene to remove physisorbed **2**, followed by repeated washing with chlorobenzene and dichloromethane.

Electrochemical measurements of **8**, **1**, and **2**

Cyclic voltammetry was carried out on an AUTOLAB (PGSTAT 10, Eco Chemie, Netherlands) electrochemical analyzer using the conventional three-electrode system of a platinum working electrode (1.6-mm-diameter disk, Bioanalytical Systems, Inc.), a platinum counter wire electrode (5-cm length of 0.5-mm-diameter wire), and a Ag/Ag⁺ reference electrode (0.1 M AgNO₃/Ag in acetonitrile with a VycorTM salt bridge). All measurements were performed at ambient temperature under nitrogen atmosphere in a dry, deoxygenated 0.1 M chlorobenzene solution of [(*n*-Bu)₄N]ClO₄. The concentration of the compounds was $\sim 3 \times 10^{-4}$ M. All potentials were referenced to the standard ferrocene/ferrocenium (Fc/Fc⁺).

Electrochemical measurements of SAM

Cyclic voltammetry was carried out using an AUTOLAB (PGSTAT 10, Eco Chemie, Netherlands) electrochemical analyzer with a conventional three-electrode system of a modified ITO working electrode (electrode area 0.36 cm²), a platinum counter wire electrode (5-cm length of 0.5-mm-diameter wire), and a Ag QRE reference electrode. All measurements were performed at ambient temperature under nitrogen atmosphere in dry 0.1 M dichloromethane solution of [(*n*-Bu)₄N]PF₆. All potentials were referenced to the standard ferrocene/ferrocenium (Fc/Fc⁺). Surface coverage was calculated using the real surface areas of the electrodes, which were determined by the electrochemical method based on mass transfer and adsorption processes.

Photoelectrochemical measurements

Photoelectrochemical measurements were performed in a designed Teflon cell. The cell was illuminated with monochromatic excitation light through a monochromator (Thermo Oriel, model 77250) by a 300-W xenon lamp (Thermo Oriel, model 6259) on a SAM of 0.36 cm². The photocurrent was measured in a three-electrode arrangement (AUTOLAB, PGSTAT 10): a modified ITO working electrode, a platinum wire counter electrode, and a Ag/AgCl (3 M NaCl) reference electrode. Light intensity was monitored by an optical power meter (Anritsu ML9002A) and corrected. Quantum yields were calculated based on the number of photons absorbed by the chromophore on the ITO electrodes at each wavelength using the input power, the photocurrent density, and the absorbance determined from the absorption spectrum on the ITO electrode.

Acknowledgments

This work was supported by the Incheon National University (501100002628) Research Grant in 2012.

Appendix A. Supplementary data

Supplementary data related to this article can be found at <http://dx.doi.org/10.1016/j.jorganchem.2014.02.022>.

References

- [1] M.R. Wasielewski, *Chem. Rev.* 92 (1992) 435.
- [2] D. Gust, T.A. Moore, A.L. Moore, *Acc. Chem. Res.* 34 (2000) 40.
- [3] F. D'Souza, O. Ito, *Chem. Soc. Rev.* 41 (2012) 86.
- [4] D.M. Guldi, C. Luo, M. Prato, A. Troisi, F. Zerbetto, M. Scheloske, E. Diel, W. Bauer, A. Hirsch, *J. Am. Chem. Soc.* 123 (2001) 9166.
- [5] H. Imahori, H. Yamada, D.M. Guldi, Y. Endo, A. Shimomura, S. Kundu, K. Yamada, T. Okada, Y. Sakata, S. Fukuzumi, *Angew. Chem. Int. Ed.* 41 (2002) 2344.
- [6] L. Sánchez, M. Sierra, N. Martín, A.J. Myles, T.J. Dale, J. Rebek, W. Seitz, D.M. Guldi, *Angew. Chem. Int. Ed.* 45 (2006) 4637.
- [7] D.I. Schuster, K. Li, D.M. Guldi, A. Palkar, L. Echegoyen, C. Stanisky, R.J. Cross, M. Niemi, N.V. Tkachenko, H. Lemmetyinen, *J. Am. Chem. Soc.* 129 (2007) 15973.
- [8] D.M. Guldi, M. Maggini, G. Scorrano, M. Prato, *J. Am. Chem. Soc.* 119 (1997) 974.

- [9] M. Fujitsuka, N. Tsuboya, R. Hamasaki, M. Ito, S. Onodera, O. Ito, Y. Yamamoto, *J. Phys. Chem. A* 107 (2003) 1452.
- [10] G.A. Rajkumar, A.S.D. Sandanayaka, K.-I. Ikeshita, Y. Araki, Y. Furusho, T. Takata, O. Ito, *J. Phys. Chem. B* 110 (2006) 6516.
- [11] K. Matsumoto, M. Fujitsuka, T. Sato, S. Onodera, O. Ito, *J. Phys. Chem. B* 104 (2000) 11632.
- [12] F. D'Souza, R. Chitta, A.S.D. Sandanayaka, N.K. Subbaiyan, L. D'Souza, Y. Araki, O. Ito, *J. Am. Chem. Soc.* 129 (2007) 15865.
- [13] I. Hiroshi, H. Kiyoshi, A. Tsuyoshi, A. Masanori, T. Seiji, O. Tadashi, S. Masahiro, S. Yoshiteru, *Chem. Phys. Lett.* 263 (1996) 545.
- [14] C. Luo, D.M. Guldi, H. Imahori, K. Tamaki, Y. Sakata, *J. Am. Chem. Soc.* 122 (2000) 6535.
- [15] H. Imahori, D.M. Guldi, K. Tamaki, Y. Yoshida, C. Luo, Y. Sakata, S. Fukuzumi, *J. Am. Chem. Soc.* 123 (2001) 6617.
- [16] H. Imahori, Y. Sekiguchi, Y. Kashiwagi, T. Sato, Y. Araki, O. Ito, H. Yamada, S. Fukuzumi, *Chem. Eur. J.* 10 (2004) 3184.
- [17] C.Y. Lee, J.K. Jang, C.H. Kim, J. Jung, B.K. Park, J. Park, W. Choi, Y.-K. Han, T. Joo, J.T. Park, *Chem. Eur. J.* 16 (2010) 5586.
- [18] F. D'Souza, O. Ito, *Coord. Chem. Rev.* 249 (2005) 1410.
- [19] H. Imahori, K. Tamaki, D.M. Guldi, C. Luo, M. Fujitsuka, O. Ito, Y. Sakata, S. Fukuzumi, *J. Am. Chem. Soc.* 123 (2001) 2607.
- [20] T. Akiyama, H. Imahori, A. Ajawakom, Y. Sakata, *Chem. Lett.* 25 (1996) 907.
- [21] H. Yamada, H. Imahori, Y. Nishimura, I. Yamazaki, T.K. Ahn, S.K. Kim, D. Kim, S. Fukuzumi, *J. Am. Chem. Soc.* 125 (2003) 9129.
- [22] H. Imahori, H. Norieda, H. Yamada, Y. Nishimura, I. Yamazaki, Y. Sakata, S. Fukuzumi, *J. Am. Chem. Soc.* 123 (2000) 100.
- [23] A. Ikeda, T. Hatano, S. Shinkai, T. Akiyama, S. Yamada, *J. Am. Chem. Soc.* 123 (2001) 4855.
- [24] S. Kang, T. Umeyama, M. Ueda, Y. Matano, H. Hotta, K. Yoshida, S. Isoda, M. Shiro, H. Imahori, *Adv. Mater. (Weinheim, Ger.)* 18 (2006) 2549.
- [25] T. Hasobe, H. Imahori, P.V. Kamat, T.K. Ahn, S.K. Kim, D. Kim, A. Fujimoto, T. Hirakawa, S. Fukuzumi, *J. Am. Chem. Soc.* 127 (2004) 1216.
- [26] Y. Matsuo, K. Kanaizuka, K. Matsuo, Y.-W. Zhong, T. Nakae, E. Nakamura, *J. Am. Chem. Soc.* 130 (2008) 5016.
- [27] Y.-J. Cho, H. Song, K. Lee, K. Kim, J. Kwak, S. Kim, J.T. Park, *Chem. Commun.* (2002) 2966.
- [28] Y.-J. Cho, T.K. Ahn, H. Song, K.S. Kim, C.Y. Lee, W.S. Seo, K. Lee, S.K. Kim, D. Kim, J.T. Park, *J. Am. Chem. Soc.* 127 (2005) 2380.
- [29] C.Y. Lee, B.K. Park, J.H. Yoon, C.S. Hong, J.T. Park, *Organometallics* 25 (2006) 4634.
- [30] C. Brückner, V. Karunaratne, S.J. Rettig, D. Dolphin, *Can. J. Chem.* 74 (1996) 2182.